J. Fluid Mech. (1980), *vol.* 99, *part* 3, *pp.* 619–640
Printed in Great Britain

Wave formation and heat transfer at an ice–water interface in the presence of a turbulent flow

By R. R. GILPIN, T. HIRATA† AND K. C. CHENG

Department of Mechanical Engineering,
University of Alberta, Edmonton, Canada

(Received 4 September 1979)

Under some conditions of temperature and flow an ice–water interface in the presence of a turbulent stream has been observed to be unstable. In this paper the source and the conditions for the instability were investigated for a well-defined turbulent boundary-layer flow. It was found that the instability resulted from the interaction that occurs between a wavy surface and a turbulent flow over it. Such an interaction results in a heat transfer variation which is 90 to 180 degrees out of phase with the surface wave shape – a result which is consistent with the calculations of Thorsness & Hanratty (1979*a*, *b*).

The main factor controlling damping of the instability at an ice–water interface was found to be the rate at which heat is conducted away from the interface into the ice.

In the past it has been found that when an ice layer is melting, that is when the heat conduction in the ice is small, the ice surface is highly unstable. In the present study it was found that for a sufficiently large temperature ratio $(T_f - T_w)/(T_\infty - T_f)$, a steady-state ice layer is also unstable. Furthermore it is predicted, from the present observations, that a growing ice layer with a ratio of ice-side to water-side heat fluxes of up to 2·3 could be unstable.

Under sufficiently unstable conditions waves on the ice surface grow to an amplitude at which flow separations occur near the wave crests. This results in a 'rippled' ice surface pattern very similar to the patterns observed on mobile bed surfaces (Kennedy 1969) or surfaces which are being dissolved into a flowing stream (Allen 1971). The development of a 'rippled' ice surface results in a very substantial increase in the mean heat-transfer rate which would have an important influence on predictions of ice formation in the presence of a turbulent stream.

1. Introduction

Problems involving phase change in which convection is occurring in the melt have received much attention in recent years. The formation of an ice cover on a river, the freezing of a water pipe, and the solidification of a metal ingot are a few of the applications in which an understanding of the interaction between phase change and convection is required.

There are a number of aspects of these problems that may cause difficulties for

† Present address: Department of Mechanical Engineering, Shinshu University, Nagano, Japan.

0022-1120/80/4503-1570 $02.00

analysis. For example, in transient cases the moving interface makes the problem nonlinear. This nonlinear character of the problem has been the primary focus of analytical studies of phase change. It has been dealt with for phase change on a flat surface by Yen & Tien (1963), Libby & Chen (1965), Lapadula & Mueller (1966), Siegal & Savino (1966), Savino & Siegal (1969) and Beaubouef & Chapman (1967), and for phase change in a pipe by Zerkle & Sunderland (1968), Özisik & Mulligan (1969) and Stephan (1969). Also in the transient problems complications may result from the fact that the specific volumes of the solid and liquid phases are seldom the same. As a result phase change at an interface is equivalent to a suction or blowing at the heat-transfer surface which may alter the heat-transfer coefficient. Merk (1954), Yen & Tien (1963), Savino, Zumdieck & Siegel (1970) and Pozvonkov, Shurgalskii & Akselrod (1970) have studied this aspect of the problem for various natural and forced convection geometries. Generally it has been found that, if the Stefan number $St = C\Delta T/L$, where C is the specific heat of the liquid, ΔT is the characteristic temperature difference in the liquid and L is the latent heat of fusion, is less than about 0·1, the heat-transfer coefficient is not significantly altered. For many ice formation problems the Stefan number is less than this value.

In problems that involve convective heat transport to a phase-change interface another interesting complication can arise from the fact that the shape of the heat-transfer surface, that is the ice–water interface, is a dependent variable which is determined by the variation of the heat-transfer rate over the surface. This means that a mutual interaction can occur among the shape of the phase-change interface, the flow field over it, and the heat-transfer rate from the liquid to the interface. This interaction can occur at steady state as well as under transient conditions. Generally in theoretical analysis of phase-change problems this interaction is minimized by assuming that the ice layer is thin enough that to a first approximation it does not affect the flow field. The interaction has, however, been analysed for some laminar flow problems such as ice formations near the leading edge of a plate (Hirata, Gilpin, Cheng & Gates 1979), in a parallel plate channel (Cheng & Wong 1977), in a pipe (Stephan 1968), and for the case of a water jet penetrating a block of ice (Gilpin & Lipsett 1978). Various problems which involve the interaction of free convection and the shape of a solidification front have also been treated (Kroegen & Ostrach 1974; Sparrow, Patanka & Ramadhyani 1977; Bathelt, Viskanta & Leidenfrost 1979). For these laminar-flow problems experimental observations, where available, have generally confirmed the theoretical predictions.

In addition to the above laminar-flow problems theoretical predictions have been made for some geometries in which a turbulent flow is assumed to exist in the melt (Genthner 1969; Shibani & Özisik 1977*a*, *b*; Thomason, Mulligan & Everhart 1978). In the turbulent flow predictions, as was done in the laminar flow cases, it is tacitly assumed that a 'smooth' and stable interface will exist. Experimental observations are much more limited for flows near or above transition Reynolds numbers; however, where such observations have been made they indicate that the interaction of shape and flow is much stronger than in the laminar case and may result in unstable or otherwise unpredicted interface phenomena. For example Hirata, Gilpin & Cheng (1979) have observed that this interaction results in the formation of a flow separation and a step change in ice thickness at the transition point for flow over an ice layer grown on a cold plate. In that study the transition point was observed to migrate

upstream on the plate to a position for which the Reynolds number was as much as an order of magnitude less than the transition point for a non-phase-change surface. The ice morphology in a pipe with flow near or above the transition Reynolds number is even more complex. In that case Gilpin (1979) has observed that the ice forms in bands such that the flow passage has successive undulations in cross-section along the length of the pipe. Each ice band has a tapered upstream section which terminates in a flow separation and a sharp increase in flow cross-section.

Of direct relevance to the present problem are observations by Ashton (1972) and Hsu (1973) that an originally flat ice slab when melted by a turbulent channel flow develops a wavy or rippled surface. Their work was motivated by the observations of Carey (1966), Larsen (1969), and Ashton & Kennedy (1972) that showed that the bottom surface of ice covers on rivers often have a wavy nature.

Melting interface instabilities are also observed in studies related to heat shield ablation (Edling & Ostrach 1970; Nachtsheim & Hagen 1972). This problem is somewhat different in that three phases are present: a solid, a liquid film, and a flowing gas. For these problems the hydrodynamic instability of the film may be partially responsible for the observed behaviour. The ablation of a phase-change surface by direct sublimation into a turbulent air stream is, however, very similar to the present problem. John & Klapa (1968) have noted the 'scalloped' surface pattern that results when snow or ice is ablated in this way.

There are two types of interface instability not related to phase-change phenomena which appear to be very similar to the instability at an ice–water interface. These are the ripple formation on a mobile bed surface and on a surface that is being dissolved into a flowing stream. Larsen (1969) and Kennedy (1969) have pointed out that the ripple patterns that occur on an ice–water interface and those that occur at low velocities on a mobile-bed surface are very similar in wavelength, in wave profile, and in the fact that the ripple pattern in both cases migrates slowly downstream with time. The surface of a dissolving solid also shows many of the same types of features (Allen 1971; Blumberg & Curl 1974).

One might suspect that the similarity that exists among these three instability phenomena results from an analogy that exists among shear stress, mass transfer, and heat transfer for turbulent flow over a wavy surface. The analogy is, however, not a simple one in that each type of instability has its own peculiarities.

In the case of a mobile bed, fluctuations in the surface shear stress are generally attributed with causing the growth of surface perturbations. Theoretical and experimental studies of the shear-stress distribution over a wavy surface (Kendall 1970; Zilker, Cook & Hanratty 1977) have, however, shown that the phase shift between shear stress and the surface profile is less than 90 degrees whereas for the shear stress itself to cause the instability a phase shift of more than 90 degrees is required. Kennedy (1969) has attributed the additional phase shift to a lag time between the increase in shear stress and the corresponding increase in bed transport. An alternative explanation is that the fluctuating component of surface pressure may have an influence on the saltation rate. In this regard the analysis of the instability of a phase change or a dissolving surface may be somewhat simpler in that the complex physics of particle saltation is not involved.

It is only in the case of instability on a phase-change surface that the growth of a small-amplitude wave into a ripple pattern has been observed. In the case of a

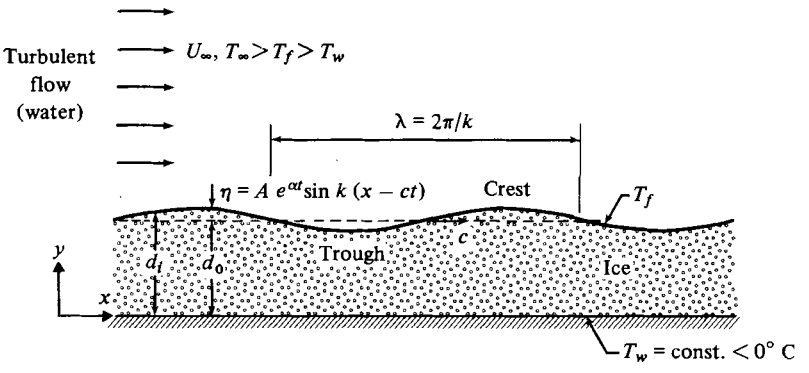

FIGURE 1. A schematic diagram of a wavy ice surface showing the definition of the symbols employed in the analysis.

dissolving surface it has been suggested that a flow separation is required before the disturbance can grow (Allen 1971). It would therefore appear that of the three similar types of instability the instability on a phase-change surface is most amenable to a comparison of theory and experiment.

To explain the growth of a wave disturbance on an ice surface a mechanism must be found by which the heat-transfer rate at the crests of the waves could be smaller than that in the valleys. This is equivalent to the requirement that the phase shift between the heat-transfer coefficient and the surface wave profile is greater than 90 degrees. Thorsness & Hanratty (1979*b*) predict such a phase shift from calculations of heat transfer in a turbulent flow over a wavy surface.

In this paper the stability and subsequent wave growth of disturbances to an ice–water interface in the presence of a turbulent boundary-layer flow will be studied experimentally. By observing the instability in the presence of a well-defined flow regime the character and stability criterion for the waves can be accurately compared with predictions.

2. Stability of an ice surface

The general features of the physical system to be considered are shown in figure 1. A turbulent stream of velocity U_∞ and temperature T_∞ flows over an ice layer. The ice layer, of mean thickness d_0, is bounded by a cold surface at T_w on one side and by the ice–water interface at T_f on the other. The interface is assumed to be perturbed such that the local thickness of the ice layer, d_i, is given by $d_i = d_0 + \eta$, where the perturbation η is expressed as

$$\eta = A\, e^{\alpha t} \sin k(x - ct). \tag{1}$$

The wavenumber $k = 2\pi/\lambda$, λ is the wavelength, c is the migration velocity of the wave, α is its amplification rate, and A is its amplitude at $t = 0$. In subsequent calculations the amplitude A will be normalized using the friction velocity u^* such that $A^+ = Au^*/\nu$.

Ashton (1972) suggested that if such an interface wave exists then the convective

heat-transfer coefficient, h, at the surface can be expressed as

$$h = h_0 + h_1,$$

where h_0 is again the mean value and the perturbed quantity h_1 is given by

$$\frac{h_1}{h_0} = fA + e^{\alpha t} \sin [k(x - ct) + \phi]. \tag{2}$$

In this expression the fluctuations in the heat-transfer rate and the interface wave profile are related by the ratio of their amplitudes, f, and the phase shift, ϕ, between them. Note that the phase shift ϕ is positive if the heat-transfer variation is shifted upstream relative to the surface wave.

A heat balance at the ice–water interface is given by

$$\rho L \frac{\partial d_i}{\partial t} = k_i \left.\frac{\partial T}{\partial y}\right|_{y=d_i} - h(T_\infty - T_f), \tag{3}$$

where the properties of the ice are density ρ, heat of fusion L, and thermal conductivity k_i. If the Stefan number $C(T_f - T_w)/L$ is small the specific heat of the ice can be neglected. As a result the temperature in the ice is just given by the Laplace equation

$$\nabla^2 T = 0 \tag{4}$$

with the linearized boundary conditions

$$T = T_f - \eta \left.\frac{\partial T}{\partial y}\right|_{y=d_0}, \quad y = d_0,$$

and

$$T = T_w, \quad y = 0.$$

If the temperature T in the ice is separated into a mean T_0 and a perturbed component T_1, the solution for the temperature can be written

$$T = T_0 + T_1, \tag{5}$$

where

$$T_0 = T_w + (T_f - T_w)\, y/d_0$$

and

$$T_1 = -(T_f - T_w) \frac{\eta}{d_0} \frac{\sinh ky}{\sinh kd_0}.$$

Introducing (5) into the heat balance and extracting the mean-value terms gives

$$\frac{\rho L}{h_0 (T_\infty - T_f)} \frac{\partial d_0}{\partial t} = \frac{k_i \theta}{h_0 d_0} - 1, \tag{6}$$

where

$$\theta = (T_f - T_w)/(T_\infty - T_f).$$

It will be useful to define a growth parameter which is the ratio of the heat flux away from the interface into the ice to the heat flux from the water to the interface; $G = (k_i \theta)/(h_0 d_0)$. From (6) it is apparent that $G > 1$ indicates an ice layer that is growing, $G < 1$ indicates an ice layer that is melting and a value of $G = 1$ indicates steady state. A value of $G = 0$ would correspond most nearly to the conditions of Ashton's (1972) experiments in which the ice slab was initially raised close to a uniform temperature of 0 °C and then melted. As has been pointed out by Ashton the stability of an ice layer will depend strongly on whether it is growing or decaying.

From (3) and (5) the equation for the perturbed quantities in the heat balance is

$$\frac{\rho L}{h_0(T_\infty - T_f)}\frac{\partial \eta}{\partial t} = -\frac{h_1}{h_0} - G\frac{k\eta}{\tanh k d_0}. \tag{7}$$

Substituting (1) and (2) in (7) and applying the multiple-angle identities for sine and cosine terms results in expressions for growth rate and wave velocity

$$\alpha = \frac{h_0(T_\infty - T_f)u^*}{\rho L \nu} k^+ \left[-\frac{f\cos\phi}{k^+} - \frac{G}{\tanh k^+ u^* d_0/\nu} \right] \tag{8}$$

and

$$c = \frac{h_0(T_\infty - T_f)}{\rho L}\frac{f\sin\phi}{k^+}, \tag{9}$$

where $k^+ = k\nu/u^*$.

If $G = 0$ the amplification rate given by equation (8) will be positive if $\cos\phi < 0$. This implies that the phase shift is in the range $\frac{1}{2}\pi < \phi < \frac{3}{2}\pi$. Furthermore if the waves are to move downstream as is observed experimentally equation (9) implies that $0 < \phi < \pi$. The phase shift that would be consistent with experimental observations is therefore one which is in the range $\frac{1}{2}\pi < \phi < \pi$. Note again that this phase shift is measured in the upstream direction.

There are a number of factors that could produce this phase shift. For turbulent flow over a wavy surface the effects of both flow acceleration and streamline curvature create extra strain rates which could affect turbulence properties. Bradshaw (1973) has suggested that of these streamline curvature is most likely to be the dominate effect. This is interesting since the curvature effect by itself would create a 180 degree phase shift and thus would be a strongly destabilizing effect. Thorsness & Hanratty (1979*a*, *b*) using a model (model D) which primarily considers the effect of pressure gradients on the viscous sublayer, find that phase shifts of between 90 and 180 degrees in the upstream direction do exist for heat transfer to a wavy wall. In order to quantitatively test these predictions in the experiments to follow the migration velocity and growth characteristics of small-amplitude sinusoidal waves in an ice-water interface will be measured and used in equations (8) and (9) to calculate f and ϕ.

To analyse the experimental data in a form consistent with the theory the value of the friction velocity for a given experiment must be known. The approach that was found to be most convenient for obtaining an estimate of the friction velocity made use of the measured mean ice thickness. The Stanton number can be related to the mean ice thickness

$$St = \frac{h_0}{\rho C U_\infty} = \frac{1}{Pr}\frac{k_i}{k_w}\frac{\theta}{G}\frac{\nu}{U_\infty d_0} \tag{10}$$

and to the friction velocity

$$St = \frac{u^*/U_\infty}{U_\infty/u^* + 5[(Pr-1) + \ln(\frac{1}{6}(5Pr+1))]}, \tag{11}$$

from which the value of u^* can be calculated.

3. Experimental apparatus and procedure

3.1. *Water tunnel*

The present experiment was carried out using a closed-loop water tunnel, shown schematically in figure 2. The unique feature of this tunnel is that it contains a heat

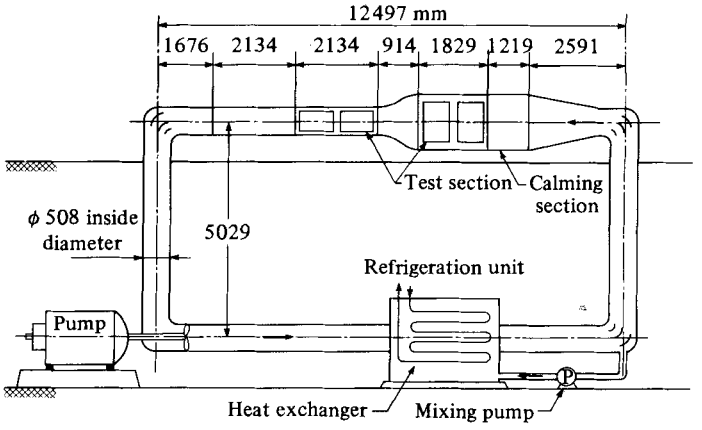

FIGURE 2. The ice–water tunnel used in the experimental studies.

exchanger connected to a refrigeration system. With this system the temperature of the water in the tunnel can be controlled at any value between room temperature and about 0·2 °C. A small, secondary circulation loop which augments the flow velocity in the heat exchanger ensures good heat exchange at low test-section velocities. The test section in which these tests were performed was 254 mm wide by 457 mm in height by 2134 mm in length. This test section had windows made of acrylic-resin plates which permitted photography of the ice surface. The tunnel was also operated in the free surface mode to facilitate probing of the boundary layer on the ice.

3.2. *The isothermal cold plate assembly*

A copper plate 6·35 mm thick, 241 mm wide, and 1520 mm long was installed horizontally in the test section with its exposed surface facing upward. The cold plate and the attached equipment are shown in figure 3. The ice was grown on the exposed upper surface of this plate. The plate was maintained isothermal and at a sub-freezing temperature by circulating a coolant fluid (a methanol–water mixture) at high velocity beneath the plate. The coolant was drawn from a large temperature-controlled bath which could be controlled at temperatures in the range 0 to − 19 °C. The temperatures of the plate, the inlet and outlet coolant, and of the bath were monitored. Owing to the high circulation rate under the plate these temperatures seldom differed by more than 1 °C.

3.3. *Formation of an ice layer*

In a typical experiment the plate and tunnel temperatures as well as the free-stream velocity would be set and the ice layer allowed to grow to its steady-state shape. For the thickest ice layers this would require 2 to 3 days. A schematic profile of an ice layer is shown in figure 3. A step in the ice profile and a small region of separated flow is shown near the leading edge of the plate. This phenomenon which occurs at the transition from laminar to turbulent flow on an ice surface was studied extensively by Hirata, Gilpin & Cheng (1979). For the range of parameters used in the present tests the 'step' transition was located 100 to 150 mm from the leading edge of the plate.

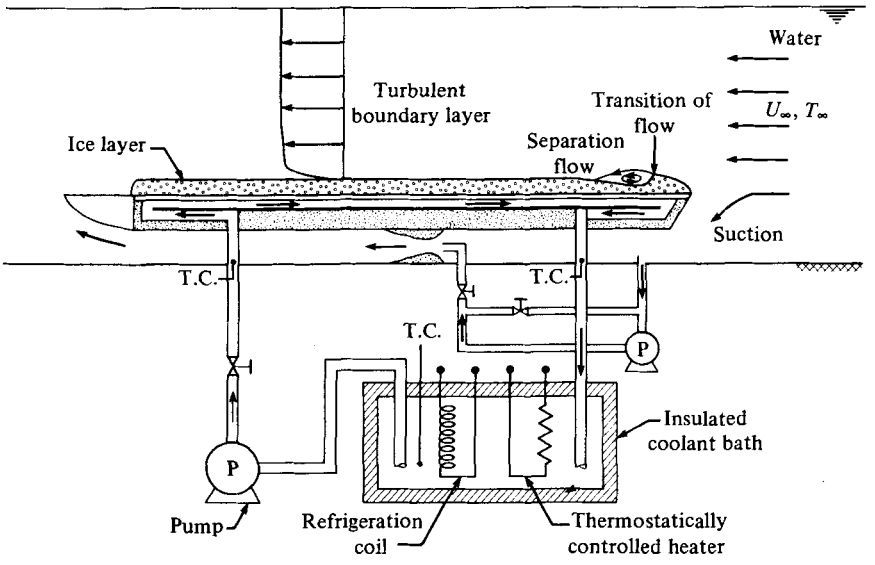

FIGURE 3. A detail of the cold plate assembly and the ice layer that forms on its surface. T.C. = Thermocouple.

Downstream of the reattachment of the separated flow a turbulent boundary layer existed. If not artificially disturbed the ice in the downstream region was normally flat and showed no sign of instability. If, however, a disturbance of sufficient amplitude was made in the ice surface the interface instability developed. Two different types of disturbances were used. In one a groove was made in the ice perpendicular to the flow direction. For most tests this groove was made by melting a 13 mm diameter, heated copper pipe half a diameter into the ice. The shape of the groove did not, however, appear to be an important factor in determining the final waveform that developed in the ice. The groove was normally made 400 to 600 mm from the leading edge of the plate so as to be well downstream of the 'step' transition. The other type of disturbance used was a sinusoidal wave several wavelengths long melted into the ice surface. Using this method the response of the surface to different wavelengths of disturbance could be observed. The amplitude of the induced disturbance was about 0·75 mm which for most of the experimental conditions studied gives a value of Au^*/ν equal to 20 to 30. Zilker *et al.* (1977) suggest that nonlinear effects become evident for waves in which Au^*/ν is greater than 27.

3.4. *Measurement of velocity, temperature and ice-shape profiles*

The velocity profiles above the wavy ice surface were measured with a laser-doppler anemometer which used an He–Ne gas laser (15 mW output) in the forward mode. Frequency shifting was employed on one of the beams to improve the doppler signal. The whole optic system was mounted on a three-axes motor-driven traversing system which was controlled by the data acquisition system. A thermocouple probe for measuring the temperature boundary layer above the ice was also mounted to the traversing head. The sensing element of the thermocouple was a copper–constantan thermocouple (76 μm diameter wire) formed in the shape of a loop about 15 mm on

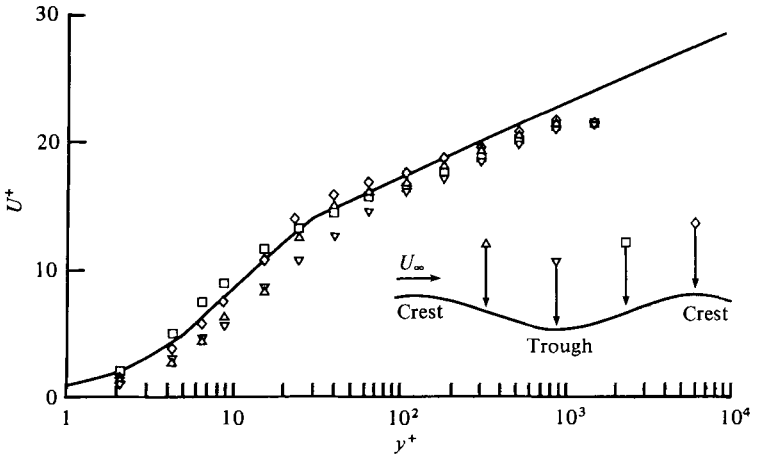

FIGURE 4. Velocity profiles at various points along the 'wavy' ice surface. $\theta = 17{\cdot}4$, $Re_\delta = 1{\cdot}1 \times 10^4$. ——, universal velocity profile.

the side. With the computer-controlled system a set of temperature and velocity profiles could be taken at various positions along the ice surface in a time which was much shorter than the time required for the shape of the ice profile to change significantly.

The profiles of the ice thickness variation along the plate were also made using the traversing system. To make these measurements a probe which followed the ice surface was traversed along the ice. The vertical displacement of this probe was detected by a linear displacement transducer. The accuracy of this system for measuring the ice interface wave amplitude and wavelength was estimated to be within ± 5 per cent.

The range of conditions employed in the present tests were:

free-stream velocity $U_\infty = 361$ to 1170 mm s^{-1},

free-stream temperature $T_\infty = 0{\cdot}4$ to $1{\cdot}07$ °C,

plate temperature $T_w = -11{\cdot}5$ to $-19{\cdot}9$ °C.

These test conditions produced Reynolds numbers based on the boundary-layer thickness $Re_\delta = 2{\cdot}5 \times 10^3$ to $5{\cdot}2 \times 10^4$ and temperature-ratio parameters $\theta_c = 7{\cdot}4$ to 44.

4. Results

4.1. *Velocity and temperature profiles*

Velocity and temperature profiles above the ice surface were measured at several positions between the crests of the small-amplitude waves occurring in near neutrally stable conditions. In figure 4 the velocity profiles are plotted in non-dimensional form u^+ versus y^+, where the mean shear velocity was used in the non-dimensionalization. The non-dimensional profiles coincide in the mean with the universal profile; however, some deviations caused by the wavy surface occur at about $y^+ = 30$. This corresponds to the outer edge of the buffer zone.

Temperature profiles taken at the same conditions as the velocity profiles are shown in figure 5. Temperatures were normalized by $\rho C u^*$. A universal temperature profile for $Pr = 13{\cdot}6$ is also shown for comparison. At this Prandtl number most of the

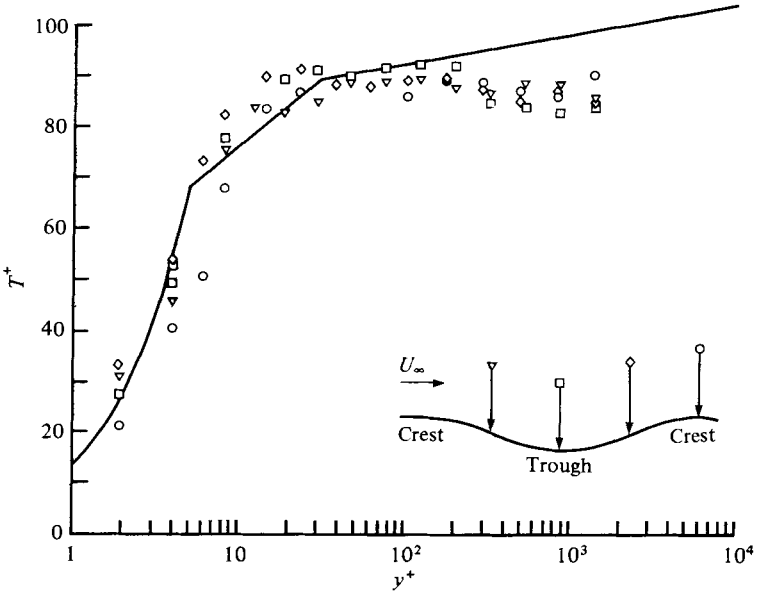

FIGURE 5. Temperature profiles above the 'wavy' ice profile. $\theta = 17{\cdot}4$, $Re_\delta = 1{\cdot}1 \times 10^4$. ——, universal temperature profile.

temperature change occurs within the laminar sub-layer which for the present experiment was of the order of 1 mm thick. This made the accurate measurement of the temperature profiles within this layer very difficult. The temperature profiles could not, therefore, be used to measure the variation in temperature gradient along the wave.

4.2. *Behaviour of small-amplitude sinusoidal disturbances*

Although the direct measurement of the variation of temperature gradient could not be used to provide quantitative data on the variation of the heat-transfer rate over a wavy surface, it was found that such information could be obtained by observing the behaviour of small-amplitude, sinusoidal disturbances melted into the ice surface. In these tests conditions of temperature and velocity near to the neutrally stable condition were chosen. The migration velocity and stability of disturbance with wavelengths shorter and longer than the most unstable wavelength was observed. Figure 6(*a*) shows the migration velocity as a function of wavenumber. In the present section we shall concentrate on the measurements made on small-amplitude disturbances (solid circles) and the measurements for large-amplitude disturbances will be discussed later. For the small-amplitude disturbances it can be seen that the migration velocity varies from negative values (that is upstream migration) for small wavenumbers to positive (downstream migration) at larger wavenumbers. In figure 6(*b*) the regions of stable and unstable behaviour are shown for the same range of disturbance wavenumbers as was used in figure 6(*a*). Also shown on this figure is the calculated damping factor $1/\tanh kd_0$ from equation (8). Note that $G = 1$ for all these tests.

At the border between unstable and stable behaviour the damping factor must be just equal to the driving force for the instability $f\cos\phi/k^+$. When these results are combined with the observed migration velocity which gives $f\sin\phi/k^+$, values of f and

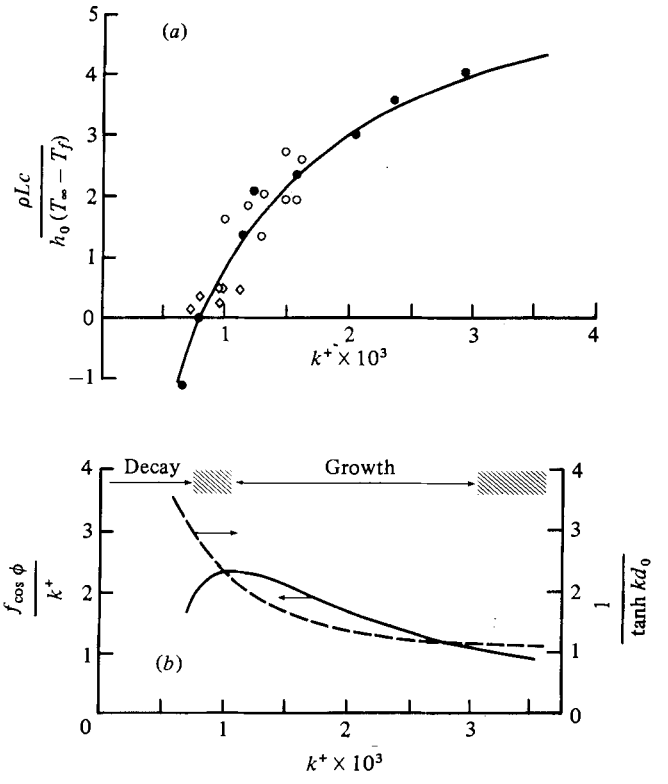

FIGURE 6. (*a*) Non-dimensionalized migration velocity of disturbances in the ice surface. ●, small sinusoidal disturbances; ○, waves downstream of a large-amplitude disturbance; ◇, ripple ice-surface pattern; ——, fitted curve for $f \sin\phi/k$. (*b*) Stability behaviour of small-amplitude disturbances. – – –, damping factor $1/\tanh(kd_0)$; ——, fitted curve for $f\cos\phi/k^+$.

ϕ can be calculated. From such tests empirical functions were obtained which provided the best overall fit to the observed velocity and stability data. These functions are

$$f = 50{\cdot}44(k^+)^{1{\cdot}435}, \tag{12a}$$

$$\phi = 758{\cdot}4 + 250{\cdot}8\ln k^+ + 23{\cdot}8(\ln k^+)^2. \tag{12b}$$

The migration velocity and instability function derived from the above empirical functions are shown in figures 6(*a*) and 6(*b*) respectively.

The values of the functions in equations (12*a*) and (12*b*) in the range of interest, $k^+ = 0{\cdot}00075$ to $0{\cdot}003$, are very similar to those predicted by Thorsness & Hanratty using their model D. Values of f are within 20 per cent and values of ϕ are within 5 degrees of the predictions of this model if a van Driest mean profile is assumed.

4.3. *Stability analysis*

With the functions f and ϕ obtained in the previous section an analysis of the stability conditions of an ice surface can be made for conditions other than those of the present experiment. Using equations (12*a*) and (12*b*) in equation (8) a prediction of the most unstable values of k^+, that is, values for which $d\alpha/dk^+ = 0$, and the neutral stability

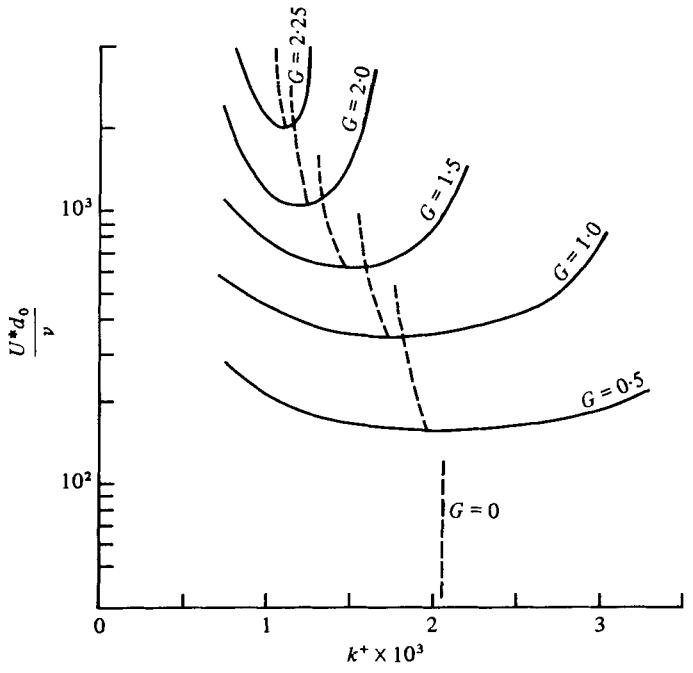

FIGURE 7. Stability curves based on linear stability theory and experimental functions for f and ϕ. --- most unstable wavenumber, ——, neutral stability condition.

condition, $\alpha = 0$, for various values of G and u^*d_0/ν can be calculated. The results are shown in figure 7.

For all conditions the most unstable wavenumbers lie between 0·00105 and 0·00205. For $G = 0$, which means there is no damping effect of the heat conduction into the ice, the most unstable wavenumber is 0·00205. In that case, however, the range of unstable wavenumbers is very large, greater than the range for which equations (12a) and (12b) are valid, and the surface is unstable regardless of the value of u^*d_0/ν. As G increases the unstable domain decreases in size. With the experimentally derived functions f and ϕ the maximum value of G for which an unstable wavenumber domain existed was a value $G = 2{\cdot}3$.

In the remainder of the paper the response of the ice surface to large-amplitude disturbances will be examined. Wavenumbers and wave speeds for the waves that result will be compared with the small-amplitude predictions.

4.4. *Growth of the ice–water interface instability from a large-amplitude disturbance*

When a groove was made in the ice surface under unstable conditions the sequence of events shown in figure 8 (a) (plate 1) occurred. In each photograph the lower light-coloured region is the ice and the upper dark region is the water. At time $t = 0$ the disturbance in the form of a semi-circular groove can be seen. As time proceeds the downstream face of the groove melts away, producing a longer groove. At the same time the ice just downstream of the groove actually thickens slightly. Further downstream about 150 mm from the original groove a second depression begins to develop at about 2 to 3 hours. This sinusoidal wave pattern spreads downstream, developing

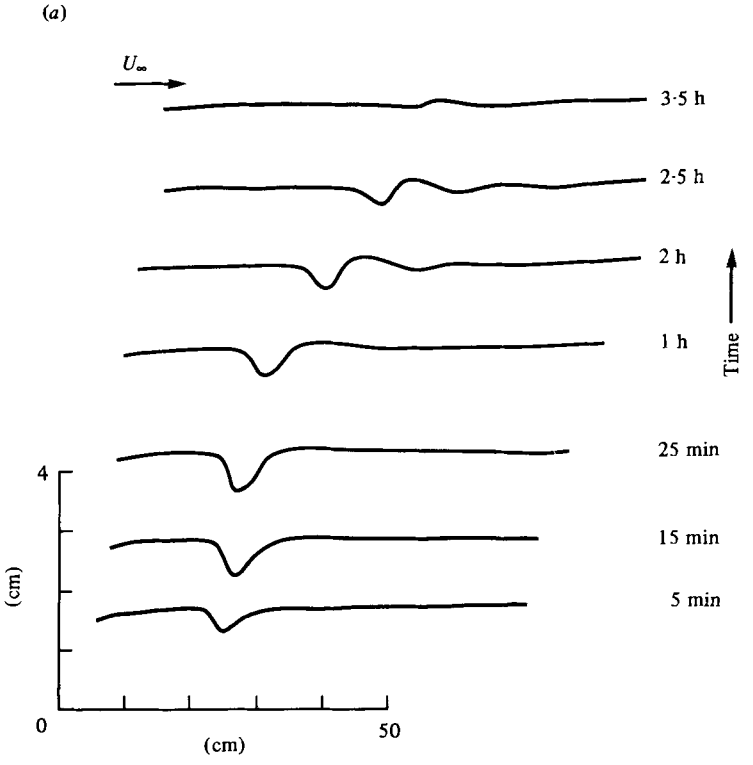

FIGURE 9 (*a*). For legend see page 634.

into a number of discernible wavelengths as time goes on. The amplitude of the waves also increases until at about $t = 3$ h the first wave downstream of the original groove 'breaks', that is, it develops a sharp crest. Subsequent waves also develop the sharp crests, at which time further changes in the wave amplitude cease. The waves do, however, continue to migrate slowly downstream. This quasi-steady wave pattern will be referred to as the 'ripple' pattern. This wave pattern is very precisely two-dimensional with the crests of the waves running perpendicular to the flow direction. Downstream of the crest of each wave is a region of separated flow. The photograph in figure 8(*b*) (plate 2) shows the flow pattern over the waves. The 'breaking' of the waves is therefore associated with the formation of a flow separation on the downstream face of sinusoidal wave.

The nature of the quasi-steady wave pattern on the ice surface depended on the velocity and temperature conditions at the ice surface. In particular it depends on the stability of the ice surface. In figure 9(*a*)–(*d*) the effects of a disturbance on an initially smooth ice surface are shown for various conditions of stability. The profiles shown in these figures were made by traversing a probe over the ice surface at various times after a groove was melted in the ice.

The ice surface was considered to be stable if it reverted to a smooth surface some time after the groove was made. This situation is shown in figure 9(*a*). Alternatively for near neutrally stable conditions, figure 9(*b*), the groove persisted and the ice downstream of the original groove took on a smooth sinusoidal ('wavy') shape. The

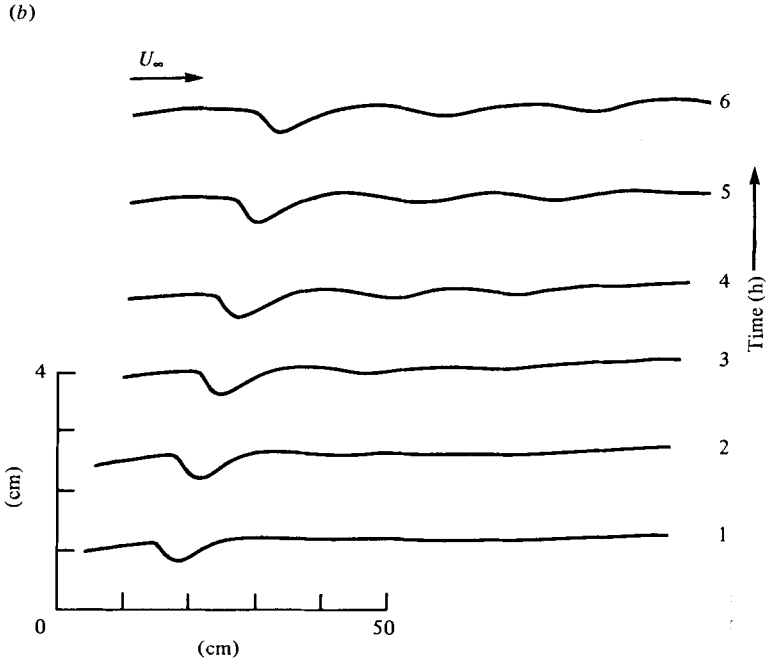

FIGURE 9 (b). For legend see page 634.

waves downstream of the original groove did not, however, grow to an amplitude at which they would induce flow separations. For a more unstable condition, figure 9(c), the downstream waves grow to a larger amplitude. It can be seen in figure 9(c) that at $t = 7$ h the waves have developed higher harmonics in their waveform as the troughs of the waves are sharper than the crests. For these conditions a flow separation or 'breaking' of the second or third wave downstream of the original groove was a common occurrence. The wave shape with just some of the waves showing a sharp crest indicative of a separated flow was called a 'partially rippled' interface. At more unstable conditions the fully developed 'ripple' interface shown in figure 8(a) was observed. Ice profiles for this condition, figure 9(d), show that a very regular series of ripples eventually develops from the original single groove. By $t = 16$ h in figure 9(d) the ripple pattern had extended the full length of the ice surface and there appears to be no reason to believe that it would not continue to propagate indefinitely downstream given a sufficient long ice surface. Even further increases in the instability of the surface resulted in a transition from a two-dimensional to a three-dimensional 'ripple' pattern. In the three-dimensional pattern the ice surface had a sculptured texture in which the wave crests formed arcs rather than straight lines.

The 'wavy' interface pattern has been reported by Ashton & Kennedy (1972) in studies of the transient melting of an ice slab in a laboratory flume. The three-dimensional ripple pattern is, however, the one most commonly reported from field observations of the bottom of ice covers (Larsen 1969, 1973; Carey 1966). This pattern has also been studied in the laboratory by Hsu (1973).

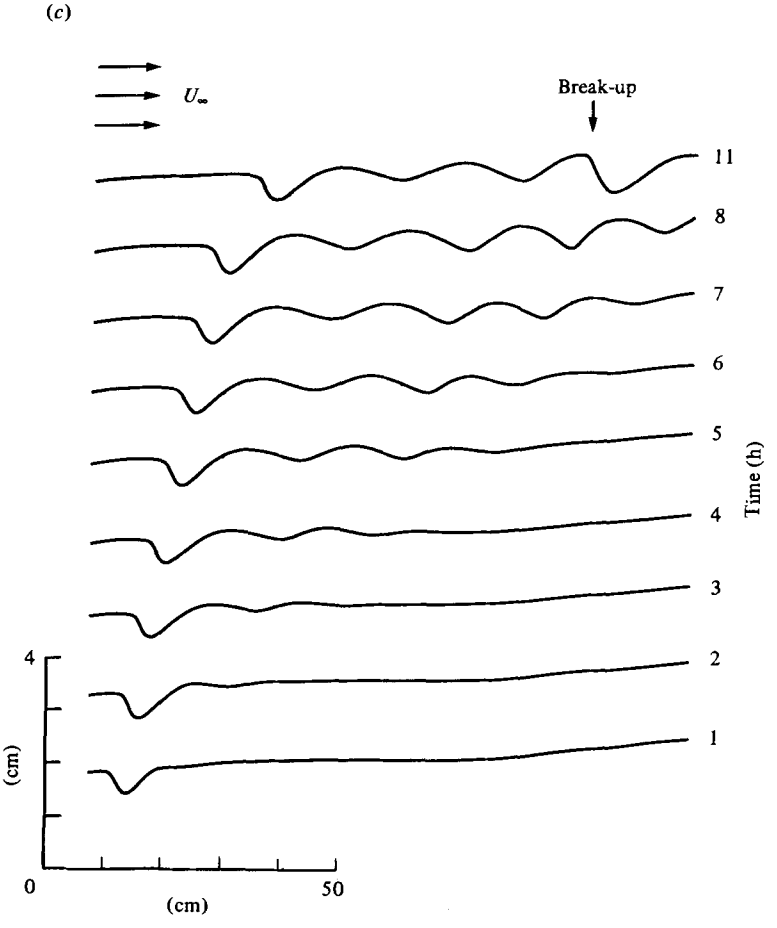

FIGURE 9 (*c*). For legend see page 634.

4.5. *Growth of large-amplitude waves*

In figure 10 the amplitude of the ice-surface waves downstream of the original groove is shown as a function of time for both the near neutrally stable and for highly unstable conditions. The amplitude of the waves has been normalized by the mean thickness of the ice layer.

For the neutrally stable conditions it can be seen that some initial growth of the wave occurs; however, their amplitude stabilizes around $A/d_0 = 0{\cdot}07$. The waveform in this case is that shown in figure 9(*b*). The non-dimensional amplitude Au^*/ν was always between 20 and 30 for these cases, which from Zilker & Hanratty (1979) should not be a large enough value for nonlinear effects to cause a cessation of growth. What appears to happen in this case is that the wavelength of the disturbances increases with time until the waves reach the lower wavenumber for neutral stability, figure 6(*b*), and this causes further growth of the wave amplitude to cease.

For the more unstable conditions where a 'ripple' pattern develops the amplitude increases more rapidly with time and obtains a larger value. The growth of higher harmonics in the waveform, as seen in figure 9(*c*, *d*), appears to be a very important

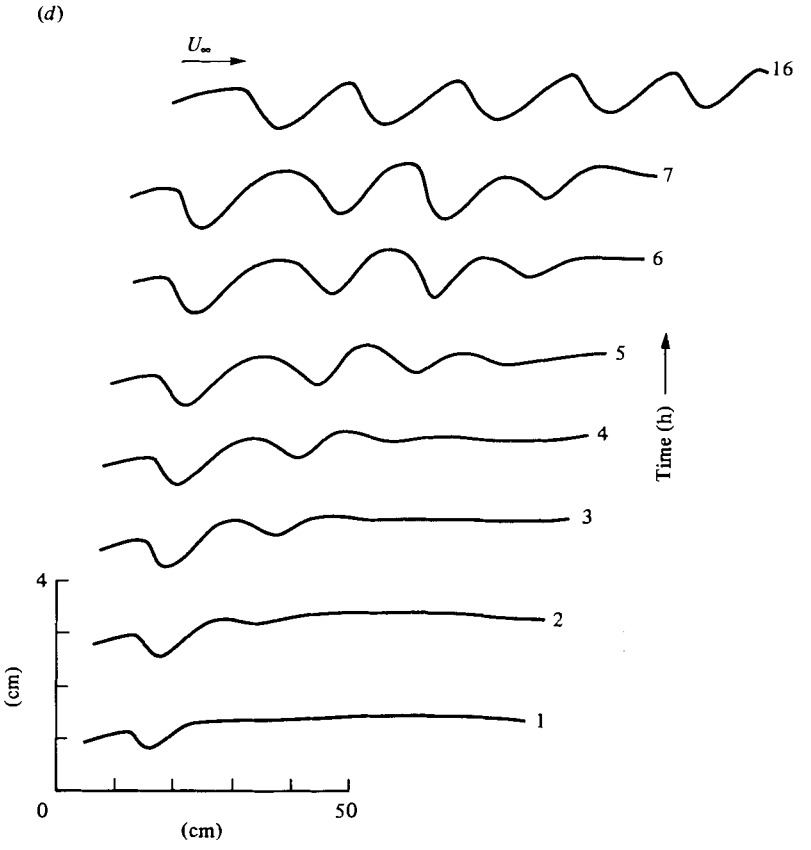

FIGURE 9. (*a*) Response of the ice surface to a large-amplitude disturbance under stable conditions $\theta = 10{\cdot}6$, $Re_\delta = 2{\cdot}5 \times 10^4$. (*b*) Development of the 'wavy' ice surface downstream of a large-amplitude disturbance under near neutrally stable conditions. $\theta = 15{\cdot}0$, $Re_\delta = 1{\cdot}4 \times 10^4$. (*c*) Development of a 'partially rippled' ice surface under somewhat unstable conditions. $\theta = 16{\cdot}8$, $Re_\delta = 4 \times 10^4$. (*d*) Development of a 'rippled' ice surface under strongly unstable conditions. $\theta = 44{\cdot}0$, $Re_\delta = 2{\cdot}6 \times 10^4$.

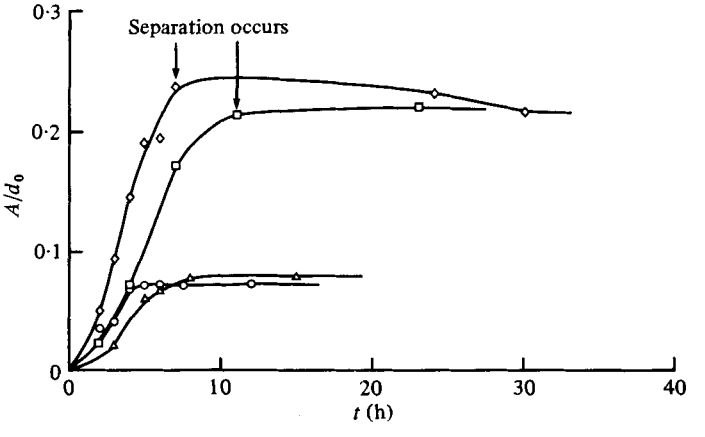

FIGURE 10. Growth of ice-wave amplitude under 'wavy' and 'rippled' ice-surface conditions. ◇, $\theta = 25{\cdot}0$, $Re_\delta = 1{\cdot}8 \times 10^4$, 'rippled'; □, $\theta = 24{\cdot}0$, $Re_\delta = 2{\cdot}6 \times 10^4$, 'rippled'; △, $\theta = 11{\cdot}9$, $Re_\delta = 2{\cdot}8 \times 10^4$, 'wavy'; ○, $\theta = 15{\cdot}0$, $Re_\delta = 1{\cdot}4 \times 10^4$, 'wavy'.

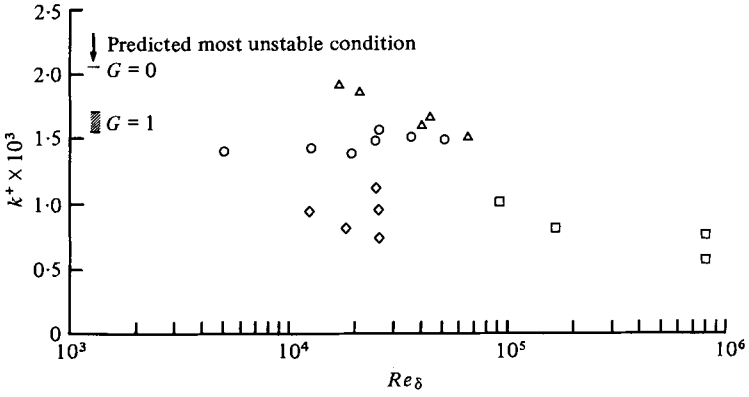

FIGURE 11. Wavenumbers of ice-surface waves under various conditions. ○, onset of 'wavy' pattern downstream of a large disturbance; ◇, fully developed 'rippled' ice-surface pattern; △, 'wavy' pattern in a flume (Ashton 1972); □, 'rippled' pattern in a river (Larsen 1973).

part of the growth of waves to these larger amplitudes. Once the waves 'break', that is, a flow separation occurs at the wave crest, the amplitude of the waves ceases to increase and may in fact decline slightly. The maximum amplitude of the 'ripple' pattern appeared to be limited to between 0·2 and 0·3 of the ice thickness.

4.6. *Wavenumber and wave speed*

The linear stability theory suggested that the wavenumbers when expressed in the form $k^+ = 2\pi\nu/(\lambda u^*)$ should be relatively insensitive to other conditions of the flow. In figure 11 the wavenumbers calculated in this form for a wide range of Reynolds numbers and from several different sources are shown. For the data from the present experiments a Reynolds number based on the measured boundary-layer thickness was used. For the flume data (Ashton 1972) and the river data (Larsen 1973) a Reynolds number based on the channel depth was employed. Also for the latter type of data the friction velocity was estimated from the empirical friction factors for channel flow. For the present experiments the onset wavenumbers of the waves created downstream of a large disturbance (open circles) agree very well with the predicted values of the most unstable wavenumbers for $G = 1$. The wavenumbers observed by Ashton (1972) for a 'wavy' ice surface in a flume are also consistent with the fact that the ice layer in those tests was decaying, that is, it was somewhere in the range $G = 0$ to 1.

The 'ripple' ice pattern in the present experiment had a significantly lower wavenumber than the 'wavy' ice pattern. This occurred not because the wavelength for a given flow condition was significantly different, but rather because the friction velocity was larger over the rough surface created by the wave. The river data for wavenumbers of the ripple pattern (Larsen 1973) again applies to a situation where G is not known but is probably in the range 0 to 1. The wavenumbers calculated for these waves are similar to those obtained in the laboratory for the 'ripple' pattern.

In figure 6(*a*) the migration velocity observed for waves resulting from large-amplitude disturbances has been plotted for comparison with the previous small-amplitude results. It appears that the migration velocity in all cases is reasonably well predicted by the small-amplitude theory. The velocity of the 'rippled' ice-surface pattern, which

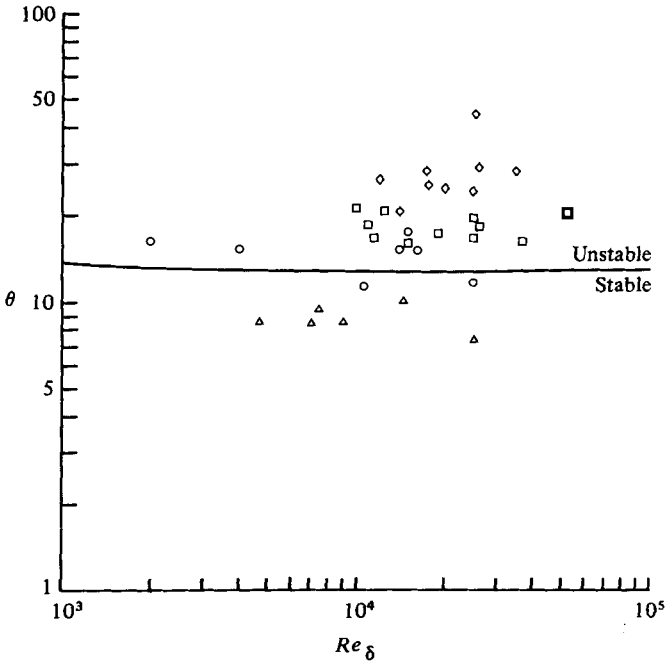

FIGURE 12. Waveforms that result from large disturbances at various stability conditions. △, stable behaviour; ○, 'wavy' ice; □, 'partially rippled' ice; ◇, 'rippled' ice; ——, stability criterion, equation (14).

is about one fifth of the velocity of the 'wavy' surface pattern, is consistent with the smaller wavenumbers that occur in the former case. These measurements are also consistent with the flume tests of Ashton (1972). Normalized in the same way the migration velocity from his observations for a 'wavy' ice surface was 2·08.

4.7. *Stability conditions*

In figure 7 the stability criterion found for a small-amplitude disturbance on a steady-state ice layer ($G = 1$) was approximately $u^*d_0/\nu = 350$. For comparison with the effects of large-amplitude disturbances it would be desirable if this condition could be translated into a condition on the more accessible parameters of temperature and Reynolds numbers. This, however, requires a knowledge of the relationship between friction velocity and Reynolds number for the unperturbed surface. In the present experiment the friction velocity was calculated from the ice thickness and the boundary-layer thicknesses were estimated from the measured velocity profiles. From these results a correlation for the friction velocity on the ice surface

$$u^*/U_\infty = 0.229 Re_\delta^{-0.132} \tag{13}$$

was obtained. Using this correlation in equations (10) and (11), the criterion for stability of a steady-state ice surface becomes

$$\theta < \frac{350(k_w/k_i)\,Pr}{4{\cdot}37 Re_\delta^{0.132} + 5[(Pr-1) + \ln(\frac{1}{6}(5\,Pr+1))]}. \tag{14}$$

In figure 12 this criterion is shown and compared with the waveforms that result

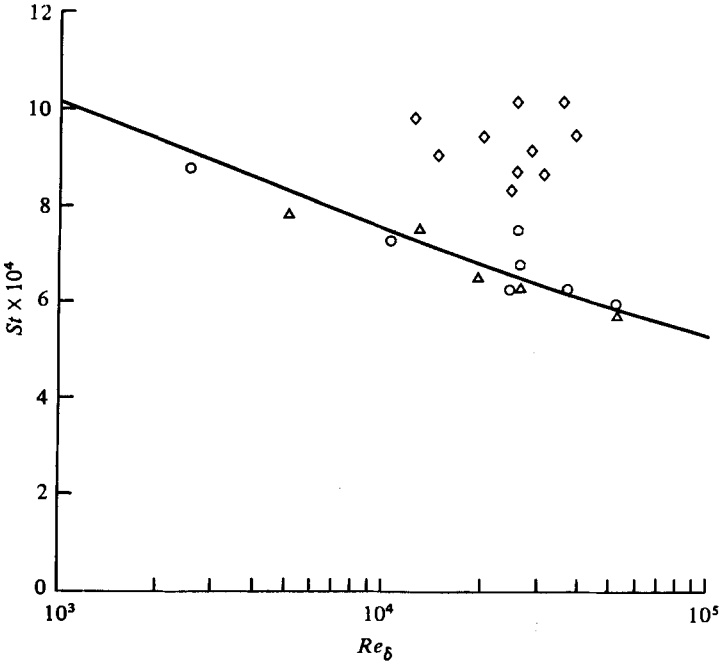

FIGURE 13. Heat transfer (Stanton number) on an ice surface. △, smooth ice; ○, 'wavy' ice; ◇, 'rippled' ice; ——, Stanton number given by empirical friction velocity, equation (13).

from a large-amplitude disturbance at various values of θ and Re_δ. From this figure it can be seen that Re_δ is not an important parameter in determining the stability and that the stability limit is approximately given by a value of the temperature parameter $\theta = 12$ regardless of Re_δ. It will also be noted that the stability limit based on small-amplitude disturbances, equation (14), is consistent with the observed behaviour of large-amplitude disturbances. This is somewhat surprising in that one might have thought that a disturbance large enough to cause a flow separation might have been unstable in a surface that would be stable for a small-amplitude disturbance. This does not appear to be the case.

4.8. *Heat-transfer rate at an ice surface*

One of the significant practical consequences of the ice-surface instability is its effect on heat-transfer rates at the ice surface. In figure 13 the Stanton number calculated from equation (10) is plotted as a function of Re_δ. The values for the undisturbed surface, which are consistent with equation (13), are shown. It can be seen that the values for the 'wavy' surface pattern are not measurably different from this. The heat-transfer rates for the rippled surface are; however, 30 to 60 per cent larger than that for the undisturbed surface. The flow separations that occur on each wave undoubtedly are responsible for this enhanced heat-transfer rate. As was noted by Hirata, Gilpin & Cheng (1979) the heat-transfer rate to the undisturbed ice surface is already 30 to 40 per cent higher than that for a flat plate of an equivalent length owing to the flow separation that occurs at the transition from laminar to turbulent flow.

5. Conclusions

An ice–water interface in the presence of a turbulent boundary-layer flow was observed to be unstable under some conditions. The dominant factor that controlled when and if an instability occurred was the heat flux from the interface into the ice. This heat flux provided the damping factor in the wave growth equation. Generally the interface is most likely to be unstable during melting, when this heat flux is small, and least likely to be unstable during ice accumulation, when the heat flux is large. Unstable behaviour was predicted, however, for conditions of ice accumulation provided the ratio of ice-side to water-side heat fluxes is less than 2·3. Under steady-state conditions where these heat fluxes are equal the temperature ratio parameter $\theta = (T_f - T_w)/(T_\infty - T_f)$, which is directly proportional to the ice-layer thickness, was found to be the controlling factor. For values of θ in excess of 12 instability was observed.

The results presented here strictly apply only for the case where a turbulent boundary-layer flow is present. Although other flows such as channel flows (Ashton 1972; Hsu 1973) and pipe flows (Gilpin 1979) have been observed to exhibit similar types of instability, the conditions for the instability to occur in these flow geometries have not been fully investigated. It may be speculated that some of the same controlling factors are important, that is, how thick the ice layer is and whether it is growing or decaying, although the specific instability conditions may vary considerably from one geometry to the next. In any case it would be highly desirable to know whether or not the interface is stable in a given problem since the existence of the instability has major consequences for efforts to develop techniques for analysing problems of phase change in the presence of a turbulent flow.

This work was supported by the Natural Sciences and Engineering Research Council of Canada.

REFERENCES

ALLEN, J. R. L. 1971 Bed forms due to mass transfer in turbulent flows: a kaleidoscope of phenomena. *J. Fluid Mech.* **49**, 49–63.

ASHTON, G. D. 1972 Turbulent heat transfer to wavy boundaries. *Proc. 1972 Heat Transfer Fluid Mech. Inst.*, pp. 200–213.

ASHTON, G. D. & KENNEDY, J. F. 1972 Ripples on underside of river ice covers. *Proc. A.S.C.E.* **98** (HY9), 1603–1624.

BATHELT, A. G., VISKANTA, R. & LEIDENFROST, W. 1979 An experimental investigation of natural convection in the melted region around a heated horizontal cylinder. *J. Fluid Mech.* **90**, 227–239.

BEAUBOUEF, R. T. & CHAPMAN, A. J. 1967 Freezing of fluids in forced flow. *Int. J. Heat Mass Transfer* **10**, 1581–1587.

BLUMBERG, P. N. & CURL, R. L. 1974 Experimental and theoretical studies of dissolution roughness. *J. Fluid Mech.* **65**, 735–751.

BRADSHAW, P. 1973 Effects of streamline curvature on turbulent flow. *AGARD* no. 169.

CAREY, K. L. 1966 Observed configuration and computed roughness of the underside of river ice, St. Croix River, Wisconsin. *U.S. Geol. Surv. Prof. Paper* 550-B, B192–198.

CHENG, K. C. & WONG, S. L. 1977 Liquid solidification in a convectively cooled parallel-plate channel. *Can. J. Chem. Engng* **55**, 149–155.

EDLING, W. H. & OSTRACH, S. 1970 An experimental study of melting wave behaviour. *Heat Transfer* 1970, vol. 1, Cu 2.3. Elsevier.

GENTHER, K. 1969 Freezing of liquids in pipes with turbulent flow. *Int. Inst. of Refrig. Bull.*, pp. 397–412.

GILPIN, R. R. 1979 The morphology of ice in a pipe at or near transition Reynolds numbers. *Heat Transfer – San Diego* 1979, A.I.Ch.E. Symposium Series 189, vol. 75, pp. 89–94.

GILPIN, R. R. & LIPSETT, A. W. 1978 Impingement melting: Experiment and numerical simulation. *Proc. 6th Int. Heat Transfer Conf.*, vol. 3, pp. 43–47. Hemisphere, Washington, D.C.

HIRATA, T., GILPIN, R. R., CHENG, K. C. & GATES, E. M. 1979 The steady state ice layer profile on a constant temperature plate in a forced convection flow: I. The laminar regime. *Int. J. Heat Mass Transfer* **22**, 1425–1433.

HIRATA, T., GILPIN, R. R. & CHENG, K. C. 1979 The steady state ice layer profile on a constant temperature plate in a forced convection flow: II. The transition and turbulent regimes. *Int. J. Heat Mass Transfer* **22**, 1435–1443.

HSU, K. 1973 Spectral evolution of ice ripples. Ph.D. thesis, Dept of Mechanics and Hydraulics, University of Iowa, Iowa City.

JAHN, A. & KLAPA, M. 1968 On the origin of ablation hollows (polygons) on snow. *J. Glaciology* **7**, 299–312.

KENDALL, J. M. 1970 The turbulent boundary layer over a wall with progressive surface waves. *J. Fluid Mech.* **41**, 259–281.

KENNEDY, J. F. 1969 The formation of sediment ripples, dunes, and antidunes. *Ann. Rev. Fluid Mech.* **1**, 147–168.

KROEGEN, D. G. & OSTRACH, S. 1974 The solution of a two-dimensional freezing problem including convection effects in the liquid region. *Int. J. Heat Mass Transfer* **17**, 1191–1207.

LAPADULA, C. & MUELLER, W. K. 1966 Heat conduction with solidification and a convective boundary condition at the freezing front. *Int. J. Heat Mass Transfer* **9**, 702–704.

LARSEN, P. A. 1969 Heat losses caused by an ice cover on open channels. *J. Boston Soc. Civ. Eng.* **56**, 45–67.

LARSEN, P. A. 1973 Hydraulic roughness of ice covers. *Proc. A.S.C.E.* **99**, 111–119.

LIBBY, P. A. & CHEN, S. 1965 The growth of a deposited layer on a cold surface. *Int. J. Heat Mass Transfer* **8**, 395–402.

MARK, H. J. 1954 The influence of melting and anomalous expansion on the thermal convection in laminar boundary layers. *Appl. Sci. Res.* **4**, 435–452.

NACHTSHEIM, P. R. & HAGEN, J. R. 1972 Observations of crosshatched wave patterns in liquid films. *A.I.A.A. J.* **10**, 1637–1640.

ÖZISIK, M. N. & MULLIGAN, J. C. 1969 Transient freezing of liquids in forced flow inside circular tubes. *J. Heat Transfer* **91**, 385–389.

POZVONKOV, F. M., SHURGALSKII, E. F. & AKSELROD, L. S. 1970 Heat transfer at a melting flat surface under conditions of forced convection and laminar boundary layer. *Int. J. Heat Mass Transfer* **13**, 957–962.

SAVINO, J. M. & SIEGEL, R. 1969 An analytical solution for solidification of a moving warm liquid onto an isothermal cold wall. *Int. J. Heat Mass Transfer* **12**, 803–809.

SAVINO, J. M., ZUMDIECK, J. F. & SIEGEL, R. 1970 Experimental study of freezing and melting of flowing warm water at a stagnation point on a cold plate. *Heat Transfer* 1970, vol. 1, Cu 2.10. Elsevier.

SHIBANI, A. A. & ÖZISIK, M. N. 1977*a* A solution of freezing of liquids of low Prandtl number in turbulent flow between parallel plates. *J. Heat Transfer* **99**, 20–24.

SHIBANI, A. A. & ÖZISIK, M. N. 1977*b* Freezing of liquids in turbulent flow inside tubes. *Can. J. Chem. Engng* **55**, 672–677.

SIEGEL, R. & SAVINO, J. M. 1966 An analysis of the transient solidification of a flowing warm liquid on a convectively cooled wall. *Proc. 3rd Heat Transfer Conf.* **4**, *A.S.M.E.*, pp. 141–151.

SPARROW, E. M., PATANKA, S. V. & RAMADHYANI, S. 1977 Analysis of melting in the presence of natural convection in the melt region. *J. Heat Transfer* **99**, 520–526.

STEPHAN, K. 1969 Influence of heat transfer on melting and solidification in forced flow. *Int. J. Heat Mass Transfer* **12**, 199–214.

THOMASON, S. B., MULLIGAN, J. C. & EVERHART, J. 1978 The effect of internal solidification on turbulent flow heat transfer and pressure drop in a horizontal tube. *J. Heat Transfer* **100**, 387–394.

THORSNESS, C. B. & HANRATTY, T. J. 1979*a* Mass transfer between a flowing fluid and a solid wavy surface. *A.I.Ch.E. J.* **25**, 686–697.

THORSNESS, C. B. & HANRATTY, T. J. 1979*b* Stability of dissolving or depositing surfaces. *A.I.Ch.E. J.* **25**, 697–701.

YEN, Y. C. & TIEN, C. 1963 Laminar heat transfer over a melting plate, the modified Leveque problem. *J. Geophys. Res.* **68**, 3673–3678.

ZERKLE, R. D. & SUNDERLAND, J. E. 1968 The effect of liquid solidification in a tube upon laminar-flow heat transfer and pressure drop. *J. Heat Transfer* **90**, 183–190.

ZILKER, D. P., COOK, G. W. & HANRATTY, T. J. 1977 Influence of the amplitude of a solid wavy wall on a turbulent flow. Part 1. Non-separated flows. *J. Fluid Mech.* **82**, 29–51.

ZILKER, D. P. & HANRATTY, T. J. 1979 Influence of the amplitude of a solid wavy wall on a turbulent flow. Part 2. Separated flow. *J. Fluid Mech.* **90**, 257–271.

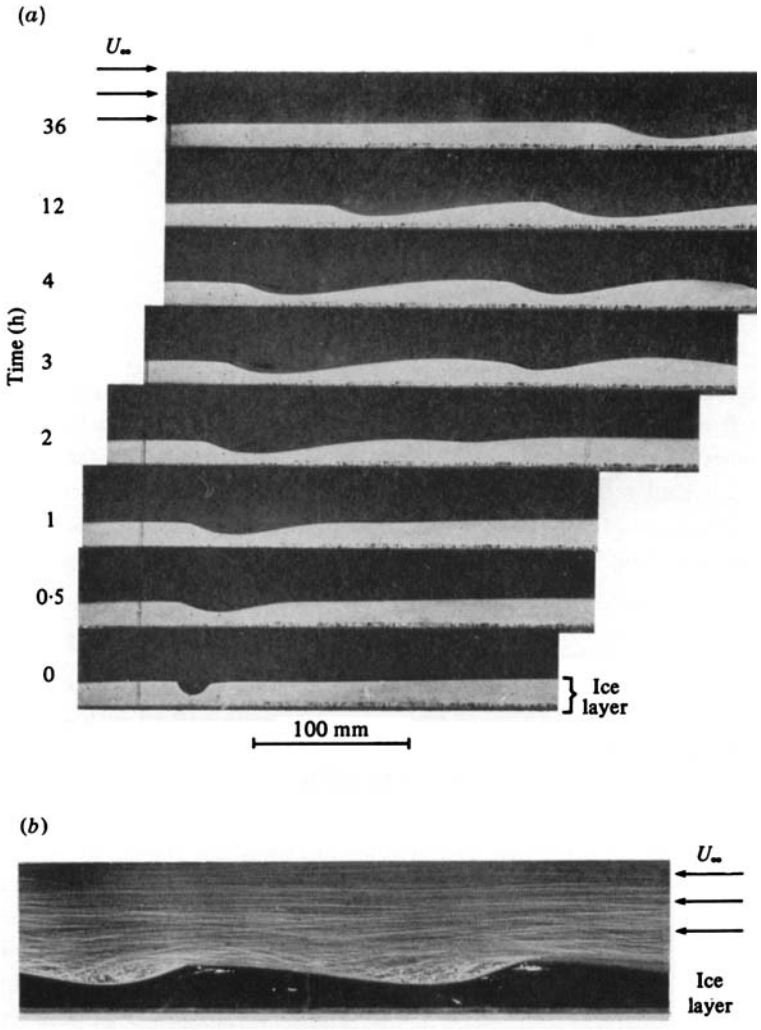

FIGURE 8. (*a*) Photographs showing the development of an ice surface wave. $\theta = 35{\cdot}6$, $Re_\delta = 4{\cdot}5 \times 10^4$. (*b*) Flow visualization over a 'rippled' ice surface. $\theta = 35{\cdot}0$, $Re_\delta = 1{\cdot}4 \times 10^4$.